*Graphical Abstract (for review)

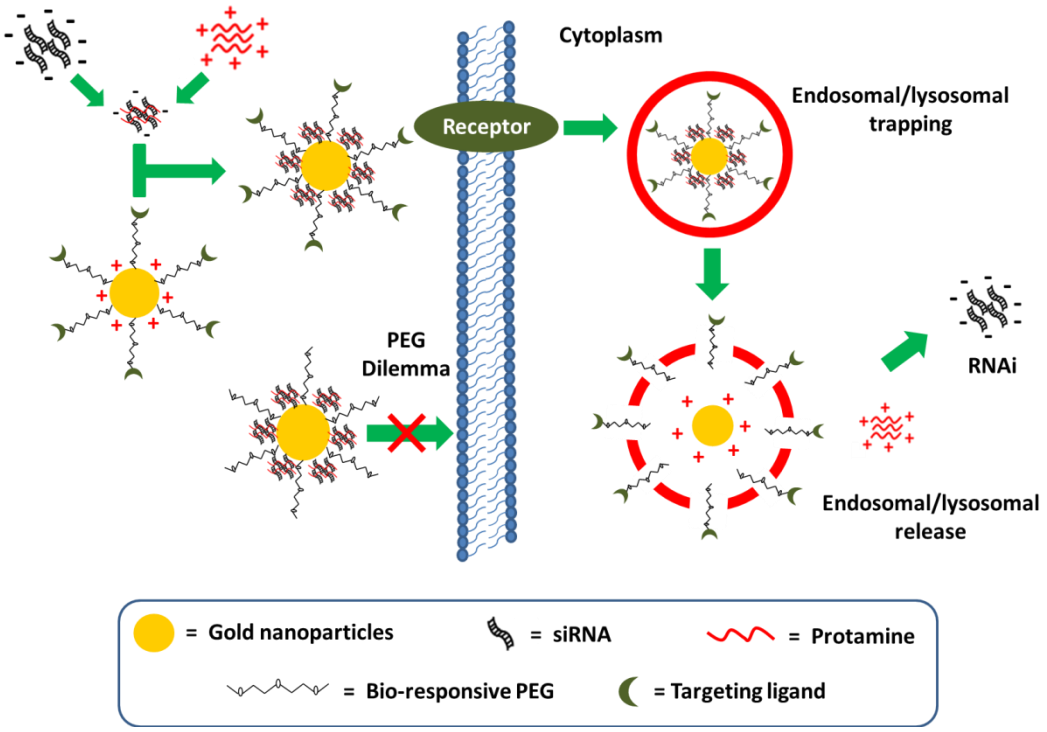

Highlights

- Positively charged, surfactant-free AuNPs capped with L-cysteine methyl ester hydrochloride conjugated to poly(ethylene glycol) (PEG) were synthesised in this study.
- PEGylated AuNPs formed nanoparticles with protamine-complexed siRNA, showing favourable physicochemical characteristics required for prolonged circulation in the blood.
- PEGylation enhanced the biocompatibility of the AuNPs and AuNP.siRNA complexation.
- PEGylation of AuNPs will facilitate conjugation of a targeting ligand to enhance cell specific uptake.

Evaluation of the physicochemical properties and the biocompatibility of polyethylene glycol-conjugated gold nanoparticles: A formulation strategy for siRNA delivery

Kamil Rahme [1, 2, 3 §], Jianfeng Guo [4 §], Justin D. Holmes [1, 2], Caitriona M. O'Driscoll [4] *

[1] Materials Chemistry and Analysis Group, Department of Chemistry and the Tyndall National Institute, University College Cork, Cork, Ireland

[2] AMBER (Advanced Materials and Biological Engineering Research Centre), CRANN (Centre for Research on Adaptive Nanostructures and Nanodevices), Trinity College Dublin, Dublin, Ireland

[3] Department of Sciences, Faculty of Natural and Applied Science, Notre Dame University (Louaize), Lebanon

[4] Pharmacodelivery group, School of Pharmacy, University College Cork, Ireland

To be submitted to: **Colloids and Surfaces B: Biointerfaces**

* To whom correspondence should be addressed

***Caitriona M. O'Driscoll**

School of Pharmacy
University College Cork
Cork
Ireland
Tel: +353-21-4901396
Fax: +353-21-4901656
E-mail: caitriona.odriscoll@ucc.ie

[§] These authors made an equal contribution to this work.

Keywords: gold nanoparticles; PEGylation; non-viral siRNA delivery; polyethylene glycol dilemma.

Abstract

The potential of RNA interference (RNAi)-based therapeutics for cancer has received much attention; however, delivery of RNAi effectors, such as small interfering RNA (siRNA), remains an obstacle to clinical translation. Non-viral delivery vectors, including cationic lipids and liposomes, polymers, cyclodextrins, peptides and metals, have been used extensively to enhance siRNA delivery. Recently, the potential of gold nanoparticles (AuNPs) for transporting drugs, proteins and genetic materials has been demonstrated. Previously, our lab has synthesised positively charged, surfactant-free AuNPs in water by the reduction of gold (III) chloride ($AuCl_3$) using hydroxylamine hydrochloride ($NH_2OH.HCl$) in the presence of L-cysteine methyl ester hydrochloride ($HSCH_2CH(NH_2)COOCH_3.HCl$) as a capping agent. These AuNPs, which achieve higher cell viability in comparison to cetyl trimethyl ammonium bromide (CTAB, a surfactant)-capped counterparts, have demonstrated potential for siRNA delivery. However, it is well known that systemic administration of cationic delivery systems without biological stablising moieties causes non-specific binding with negatively charged serum proteins, resulting in particle aggregation and opsonisation. Consequently, highly stable AuNPs capped with L-cysteine methyl ester hydrochloride ($HSCH_2CH(NH_2)COOCH_3.HCl$) conjugated to poly(ethylene glycol) (PEG) were synthesised in this study. These PEGylated AuNPs formed nanoparticles (NPs) with siRNA (which was first compacted with protamine); the complexes had a diameter within the nanoscale range (~ 250 nm), and a near neutral surface charge (~ 10 mV). PEGylation enhanced the biocompatibility of the AuNPs by reducing toxicity in a range of cell types, by inhibiting interaction with serum proteins thus avoiding aggregation, and, by providing protection against degradation by nucleases. In the future the existance of the PEG chain on the AuNPs will facilitate conjugation of a targeting ligand to enhance cell specific uptake.

1. Introduction

The availability of data obtained from sequencing the whole genome of cancer cells has resulted in significant changes to our understanding of the molecular pathogenesis of cancer [1]. This information has advanced the application of RNA interference (RNAi) by identifying sequences complementary to specific target genes, which can be used to improve drug discovery and target validation [2] and [3]. Recently, inhibiting specific gene expression by RNAi has presented a new therapeutic strategy to treat many diseases, including metabolic disorders, viral infections and cancer at the molecular level [4]. However, one of the obstacles for RNAi effectors [i.e. small interference RNA (siRNA) and microRNA (miRNA)] impeding their clinical progression is the lack of safe and efficient delivery system [4]. Non-viral delivery vectors, including cationic lipids and liposomes, polymers, cyclodextrins, peptides and metals, have been extensively used for siRNA delivery with varying degrees of success [5] [6] [7] [8] [9] [10] [11] and [12]. Among these, gold nanoparticles (AuNPs) have shown great potential as siRNA delivery vectors for the treatment of various malignancies due to favorable properties such as a bio-inert surface, easily modifiable surface chemistry and the high degree of control possible over size and shape during synthesis [13] [14] [15] and [16].

To achieve successful siRNA delivery, several studies have investigated the effect of particle size, shape, surface charge, chemical composition and formulation strategy for AuNPs on toxicity, intracellular trafficking and gene silencing [15] [16] [17] and [18]. Due to the variability of parameters used in these studies including the physicochemical properties of particles, cell types, dosing regimens and biochemical assays, however, it is difficult to identify the ideal properties of AuNP-based delivery system.

We have recently synthesised a group of different sized, nearly spherical, positively charged, surfactant-free AuNPs by a seeding growth method involving the reduction of gold (III) chloride ($AuCl_3$) using hydroxylamine hydrochloride ($NH_2OH.HCl$) in the presence of L-cysteine methyl ester hydrochloride ($HSCH_2CH(NH_2)COOCH_3.HCl$) as a capping agent [19]. These AuNPs demonstrated significantly higher cell viability (~ 3 fold) in comparison to cetyl trimethyl ammonium bromide (CTAB, a surfactant)-capped counterparts. In addition, they achieved effective complexation of siRNA and facilitated internalisation into cancer cells, indicating the potential for siRNA delivery [19]. However, prior to systemic administration these AuNPs require further development; as positively charged delivery

vectors may cause *in vivo* instability due to non-specific adsorption of plasma/serum proteins [20] and [21]. In the case of cationic vectors modifications using polyethylene glycol (PEG) have been widely empolyed to improve stability in salt and serum environments, therefore reducing interaction with plasma/serum components and prolonging blood circulation of siRNA [22].

PEGylation of a group of AuNPs capped with L-cysteine methyl ester hydrochloride ($HSCH_2CH(NH_2)COOCH_3.HCl$) through partial ligand exchange of L-cysteine by thiolated methoxy polyethylene glycol (mPEG-SH) was achieved in the present study. When these positively charged AuNPs were decorated with PEG of different molecular weights they displayed spherical morphology with a wide range of mean diameters (20-200 nm). In order to achieve an effective formulation, siRNA was first compacted with protamine, followed by complexation with PEGylated AuNPs [23]. The physicochemical propeties and the biocompatibity of the resulting formulations were evaluated.

2. Materials and methods

2.1. Materials

Purified H_2O (resistivity ≈ 18.2 MΩ cm) was used as a solvent for synthesis of AuNPs. All glassware was cleaned with aqua regia (3 parts of concentrated HCl and 1 part of concentrated HNO_3), rinsed with distilled water, ethanol, and acetone and oven-dried before use. Gold (III) chloride ($AuCl_3$), sodium borohydride ($NaBH_4$), hydroxylamine hydrochloride ($NH_2OH.HCl$) were purchased from Sigma-Aldrich. L-cysteine methyl ester hydrochloride ($HSCH_2CH(NH_2)COOCH_3.HCl$) was obtained from Fluka. Thiol terminated poly(ethylene glycol) methyl ether (mPEG-SH), M_w = 2,100, 5,400, 10,800 and 20,800 g mol^{-1} were purchased from Polymer Source®, which thereafter refer to PEG 2,000, 5,000, 10,000 and 20,000, respectively. All products were used as received.

2.2. Preparation of Gold Nanoparticles

2.2.1. Seed-Mediated Growth of Gold Nanoparticles

The AuNPs were synthesised based on a seed-mediated growth method using hydroxylamine hydrochloride as a reducing agent [24] and [25]. In a typical procedure, to an aqueous solution (50 mL) of $AuCl_3$ (0.5 mmol L^{-1}), 0.49 mL of a 51.6 mmol L^{-1} L-cysteine methyl ester hydrochloride solution was added to different volumes of the AuNPs-L-cysteine colloidal seed solution. The mixture was stirred gently. Afterwards 0.33 mL of 115.8 mmol L^{-1} $NH_2OH.HCl$ was added and the solution was stirred for a few hours (between 2 and 18 hr). Further details of the synthesis have been previously described in [19].

2.2.2. Grafting of Poly(ethylene glycol) Ligands

Thiol functionalised methoxy poly(ethylene glycol) (mPEG-SH) was covalently grafted to the surface of AuNPs through gold sulfur bond formation. A solution of mPEG-SH of the desired molecular weight was added drop wise to a solution of L-cysteine-capped AuNPs while stirring (the final concentration of mPEG-SH was fixed at 3 µmol L^{-1} for GR5 and GR7 and 5 µmol L^{-1} for GR8, GR9, GR11 and GR12). The solution was stirred for ~2 h allowing L-cysteine ligands to exchange with PEG-SH; successful attachment of PEG onto AuNPs was confirmed by DLS and Zeta potential measurements.

2.2.3. Dynamic Light Scattering

The measurements were undertaken with the Malvern instrument (Zetasizer Nano Series) at 25 °C using the default non-invasive back scattering (NIBS) technique with a detection angle of 173°. Three measurements were made per sample and the standard deviation (σ) was calculated, typically σ = 1-2 nm.

2.3. Preparation and Characterisation of Gold Nanoparticle.siRNA Complexation

The PEGylated AuNPs (100 µg mL^{-1}) were added to a solution of siRNA (the Negative Control siRNA, sense sequence 5'-UUC UCC GAA CGU GUC ACG U-3', prepared in RNase-free water following Sigma-Aldrich recommendations), at different mass ratios (MRs) of AuNPs to siRNA, followed by 1 h incubation with 300 rpm shaking at room temperature (RT).

Alternatively, protamine (Sigma-Aldrich) was added to a solution of siRNA at a MR 0.4 of protamine to siRNA, followed by 30 min incubation at RT with 300 rpm shaking.

Subsequently, AuNPs were added to 'protamine.siRNA' at different MRs of AuNPs to siRNA, followed by 30 min incubation with 300 rpm shaking.

The ability of AuNPs to complex 'protamine.siRNA' was analysed by gel retardation. In brief, complexes of AuNPs and 'protamine.siRNA' were prepared as described above and loaded onto 1% (w/v) agarose gels in Tris/Borate/EDTA (TBE) buffer (Sigma-Aldrich) containing SafeView (NBS Biologicals, UK). Electrophoresis was performed at 120 V for 30 min and the resulting gels were photographed under UV.

In addition, particle size and zeta potential were measured with the Malvern instrument (Zetasizer Nano Series). 0.01 mM NaCl (0.2 μm membrane-filtered) was added to the complexes and made up to 1 mL before measurement. The concentration of siRNA was fixed at 1 μg mL^{-1}.

2.4. Serum Stability of siRNA Complexes

Complexes containing 'protamine.siRNA' (0.5 μg AuNPs, 0.2 μg protamine and 0.5 μg siRNA, MR = 1:0.4:1) were incubated for 24 h in 50% (v/v) fetal bovine serum (FBS, Sigma-Aldrich) at 37 °C. Following incubation, samples were treated for 1 h with excess heparin (1000 IU mL^{-1}) to release the siRNA from complexes at RT and then loaded onto 1.5% (w/v) agarose gels in TBE buffer containing SafeView. Electrophoresis was performed at 120 V for 30 min and the resulting gels were photographed under UV.

In addition, these complexes (1 μg AuNPs, 0.4 μg protamine and 1 μg siRNA, MR = 1:0.4:1) were incubated in 50 % (v/v) FBS at 37 °C for 24 h and the particle size was measured using the Malvern Nano-ZS (Malvern Instruments, UK). FBS on its own and complexes incubated in deionised water (DIW, it was filtered by 0.2 μm membrane) at 37 °C for 24 h were used as controls. The concentration of siRNA was fixed at 1 μg mL^{-1}.

2.5. Cell Culture and Cytotoxicity

Hep G2 (human hepatocellular carcinoma cell line) and Caco-2 (human colorectal adenocarcinoma cell line) cells were maintained in DMEM medium (Sigma-Aldrich)

supplemented with 10 % FBS and 2 mM L-glutamine. PC-3 (human prostate carcinoma cell line), B16F10 (mouse melanoma cell line) and CT26 (mouse colon carcinoma cell line) cells were maintained in RPMI medium (Sigma-Aldrich) supplemented with 10 % FBS. These cells (passage number < 30) were grown in the incubator (ThermoForma) at 37 °C with 5 % CO_2 and 95 % relative humidity.

Cytotoxicity of AuNPs was assessed using the MTT assay with 3-(4, 5-Dimethylthiazol-2-yl)-2, 5-diphenyltetrazolium bromide (Sigma-Aldrich) [26]. Hep G2 (20,000 cells per well), Caco-2 (10,000 cells per well), PC-3 (5,000 cells per well), B16F10 (1,000 cells per well) and CT26 (6,000 cells per well) cells were seeded within 200 µl growth media in 96-well plates one day before transfection. AuNPs were incubated with cells for 24 h under normal growth conditions. Following incubation, the particle solution was replaced with 200 µl fresh growth medium, and 20 µl MTT stock (5 mg mL^{-1} in PBS) was added and incubated with cells for 4 h at 37 °C. The contents were removed and 100 µl DMSO was added to dissolve the purple formazan products. Absorbance was measured at 590 nm using a microplate reader. Results were expressed as % dehydrogenase activity compared to untreated controls.

2.6. Fluorescence Activated Cell Sorting

PC-3 cells (5 x 10^4 cells/well) were seeded in 24-well plates and incubated for 24 h under normal growth conditions. Cells were then transfected with 50 nM fluorescein-siRNA (sense sequence sense sequence 5'-UUC UCC GAA CGU GUC ACG U-3', modified by 6-FAM on 5' of sense sequence, prepared in RNase-free water following Sigma-Aldrich recommendations), 'protamine.fluorescein-siRNA' or 'protamine.fluorescein-siRNA' complexed with AuNPs, and incubated for 4 and 24 h in 10 % FBS-containing growth medium. Naked fluorescein-siRNA was used as the negative control, and siRNA complexed with Lipofectamine® 2000 (Life Technologies) (prepared following the manufacturer's recommendation) was used as the positive control. Before FACS, cells were first treated with CellScrub (Genlatins) to remove complexes associated with the cell surface (uninternalised complexes) according to manufacturer's instructions. The medium was then removed by aspiration, and cells were washed twice with PBS and trypsinised. Cells were subsequently centrifuged (1,000 rpm for 5 min), the supernatant was carefully discarded and the pellets were re-suspended in 1 mL cold PBS in Polystyrene Round-Bottom Tubes (Becton

Dickinson). Ten thousands cells were measured for each sample using the Becton Dickinson FACScalibur manual. Fluorescein-positive cells were displayed by Histogram Plot.

2.7. Statistics

One-way analysis of variance (ANOVA) was used to compare multiple groups followed by Bonferroni's post hoc test. Statistical significance was set at $*p < 0.05$.

3. Results and discussion

3.1. Synthesis and characterisation of PEGylated Gold Nanoparticles

3.1.1. Synthesis of PEGylated Gold Nanoparticles

Initially non-PEGylated L-Cysteine AuNPs with different sizes (GR5, GR7, GR8, GR9, GR11 and GR12) were synthesised as previously described [19]. Following the addition of mPEG-SH, with desired molecular weights (M_w = 2,100, 5,400; 10,800 and 20,800 g mol^{-1}), L-cysteine ligands were partially exchanged with mPEG-SH. The aim of the present study was to stabilise the AuNPs with a neutral PEG while retaining some residual positive charge on the AuNP surface to enable the final AuNP-L-cysteine-PEG to complex negatively charged siRNA. Consequently, the mPEG-SH was not added in large excess, where the concentrations of mPEG-SH were fixed at 3 µmol L^{-1} for GR5 and GR7 ([Au(0)]/[mPEG-SH] = 167) and 5 µmol L^{-1} for GR8, GR9, GR11 and GR12 ([Au(0)]/[mPEG-SH] = 100), in order to produce a 'mushroom' conformation which is known to occur at low surface density rather than a 'brush' conformation which occurs at high PEG density [22]. However, it should be noted that a possible transition of mushroom to brush conformation can take place when the size of AuNP core decreases [23]. When the resulting PEGylated AuNPs solutions were stored at 4 °C for 12 months no significant changes in size and charge were detected. In addition, attempt to determine the number of mPEG-SH per AuNPs surface and study the effect of grafting density of mPEG-SH onto AuNPs-Lcysteine on their stability, cellular uptakes and efficiency in siRNA delivery, will be performed in future study [13] [16] [27] and [28].

3.1.2. Dynamic Light Scattering

Dynamic light scattering (DLS) is a method for characterisation of nanoparticle dispersions and nanoparticle-polymer hybrids from which the hydrodynamic diameter (D_h) can be determined. PEG is a flexible linear polymer that can dramatically affect the Brownian motion of particles by introducing additional frictional drag, thus reducing nanoparticle diffusivity. Moreover, PEGylation increases the stability of AuNPs in complex media and prevents their aggregation under physiological conditions [23]. Results in Fig. 1A show the hydrodynamic diameter calculated from the size distribution by volume of the samples AuNPs-PEG 2,000 with different AuNP core size and a fixed PEG length (M_w 2,100 g mol^{-1}). The core diameter of AuNPs (namely GR5, GR7, GR8, GR9, GR11 and GR12) used in this study correspond to ~38, ~60, ~92, ~113, ~136, and ~191 nm as determined from DLS (Table 1). In Fig. 1A, the position of the peak maximum of the AuNPs-PEG 2,000 shifts from 47 nm to 196 nm when the AuNP core increases from about 38 nm to 191 nm. While the zeta potential of all AuNPs-PEG 2,000 were approximately 31 ± 2 mV due to the original positively charged AuNP core (Fig. 1B), it was noted that the zeta potential decreased by 4 to 12 mV after PEGylation indicating that the particles were coated with the PEG 2,000 (Table 1).

Results in Fig. 2A show the size distribution of GR5 AuNPs-L-cysteine before and after coating with different PEG length (M_w ~ 2,100, 5,400, 10,800 and 20,800 g mol^{-1}). An increase in the mean nanoparticle diameter from ~38 nm for 'bare' L-cysteine capped AuNPs to ~76 nm for an mPEG-SH molecular weight of 20,800 g mol^{-1} is clearly seen. The zeta potential measurements, Fig. 2B, shifted from around 35 mV for L-cysteine capped Au nanoparticles, to ~ 12 mV for AuNPs with an mPEG-SH molecular weight of 20,800 g mol^{-1} indicating the shielding of the surface charge on the nanoparticle by a coating of the neutral mPEG-SH.

The results in Table 1 highlight the zeta potentials (mV), their peak width (zeta deviation) and hydrodynamic diameters (D_h) and the polydispersity index (PDI) of all the PEGylated AuNPs-L-cysteine solutions used in this study, as well as the synthesised 'bare' L-cysteine capped AuNPs prior to coating with mPEG-SH of different length. In Table 1, successful PEGylation of the AuNPs-L-cysteine can be clearly seen from the increase in size of all AuNP samples with increasing PEG length accompanied by a decrease in the zeta potential (Figs. 1, 2 and S1). In addition, PEGylated AuNPs displayed a nearly spherical morphology

(TEM data shown in S2) which was similar to the corresponding non-PEGylated nanoparticles [19].

3.1.3. Cytotoxicity of PEGylated Gold Nanoparticles

Although AuNPs are generally recognised as nontoxic, recent reports have demonstrated that physicochemical parameters, such as particles size, surface chemistry and charged surface functional groups, play a crucial role in determining genotoxic-, mutagenic- or cell toxicity effects [29] [30] and [31]. In this study, the cytotoxicity of PEGylated AuNPs was studied in Hep G2, Caco-2, PC-3, B16F10 and CT26 cells using an MTT assay (Table 1S to 5S). Results showed that PEGylated GR5, GR7, GR8, GR9, GR11 and GR12 AuNPs displayed higher cell viability (50% cell growth inhibition, IC50 ≈ 7 to 15 μg mL^{-1}) in comparison with their non-PEGylated counterparts (IC50 ≈ 7 to 9 μg mL^{-1}) as previously reported [19]. It is also interesting to note that AuNPs-L-cysteine with longer PEG chains demonstrated less cytotoxicity compared to those with shorter PEG (i.e. in the PC-3 cell line, GR11 with PEG 2,000, 5,000, 10,000 and 20,000 displayed IC50 values equal to 8.7, 11.5, 13.8 and 15.9 μg mL^{-1}, respectively) (Table 1S to 5S). Therefore, G11 AuNPs PEG 20,000 (Fig. S1) was selected for complexation with 'protamine.siRNA' in all further experiments (unless otherwise mentioned).

3.2. Formation and characterisation of PEGylated Gold Nanoparticle.siRNA complexation

3.2.1. Complexation of siRNA with PEGylated Gold Nanoparticles

Previous results have shown that efficient complexation of siRNA with non-PEGylated Cysteine GR11 AuNPs occurred from MR20 onward via electrostatic interaction [19]; in contrast, PEGylated GR11 AuNPs-L-cysteine failed to complex siRNA (Fig. S3). This is most likely due to that fact that PEGylation may reduce the zeta potential and surface area of AuNPs, therefore impairing the complexation with siRNA [22] and [32].

Protamine, a highly positive charged peptide, has been used as a condensation reagent for nucleic acids to improve transfection efficiency [25] and [33]. In order to achieve efficient siRNA complexation with the PEGylated AuNPs, protamine was first used to partially complex siRNA (Fig. S4). As the overall surface charge of 'protamine.siRNA' at MR 0.4

remained negative (~ -25 mV), it was selected for further complexation to the slightly cationic PEGylated G11 AuNPs. Results showed that the 'protamine.siRNA' was effectively complexed with PEGylated G11 (Fig. 3).

The size and charge of complexes formed between siRNA, protamine and AuNPs were measured by DLS. The data showed that negatively charged 'protamine.siRNA' was electrostatically complexed with PEGylated G11 resulting in new formulations with a nano-scale particle size (~ 250 nm) and a slightly positive surface charge (~ 10 mV) (Fig. S5). It is interesting to note that when the mass ratio of PEGylated G11 and siRNA was increased above 4:1 the particle size and surface charge did not change significantly (Fig. S5).

It has been reported that systemically administrated NPs can accumulate into tumour tissues via the 'enhanced penetration and retention' (EPR) effect, in which the immature and leaky vasculature provides access to circulating particles with diameter less than 500 nm [20]. The average hydrodynamic diameter (~ 250 nm) of PEGylated complexes suggests that they could enter solid tumours through the EPR effect.

3.2.2. Serum stability of PEGylated Gold Nanoparticle.siRNA Complexes

Systemically administrated gene delivery vectors face a set of obstacles before reaching target cells. These include non-specific uptake by the reticuloendothelial system (RES), in which NPs are rapidly removed from the bloodstream into the liver, spleen or bone marrow [34]. One strategy to overcome this is to chemically graft PEG moieties, which can mask positively charged surfaces, onto cationic NPs thereby stabilising the complexes against salt, protein and complement-induced instability [22]. It has been demonstrated that AuNPs functionalised with PEG are stable in biological media. For instance, PEGylation of AuNPs significantly improved nanoparticle stability in water, PBS solution, PBS containing bovine serum albumin (BSA) and dichloromethane (DCM) [35].

In the current study, particle size distribution data generated from DLS measurements demonstrated that aggregation (> 1 µm) occurred when complexes of non-PEGylated G11 and 'protamine.siRNA' (MR = 8:0.4:1) (~ 30 mV) were incubated in 50 % FBS at 37 °C for 24 h (Fig. 4A). In contrast, complexes of G11 PEG 20,000 and 'protamine.siRNA' (MR = 8:0.4:1) resisted to aggregation for up to 24 h under the same conditions (Fig. 4B). *In vitro* aggregation studies have been shown to accurately predict the *in vivo* performance of NPs

[36]; consequently the lack of aggregation seen in the current work suggests that the PEGylated AuNPs have potential to prolong circulation of siRNA in the blood.

In addition, it has been reported that naked siRNA is degraded in plasma with a half-life of minutes [20]. However, formulations with various delivery vectors can protect siRNA against serum-mediated degradation. To verify whether Au complexes containing 'protamine.siRNA' are able to protect siRNA from serum nucleases, naked siRNA, 'protamine.siRNA' (MR = 0.5, in which complete siRNA complexation was generated, Fig. S4) and 'G11 PEG20,000 'protamine.siRNA'' (MR = 1:0.4:1) were incubated in 50% FBS at 37 °C for 24 h. Naked siRNA and 'protamine.siRNA' were not stable following 24 h incubation (Fig. 5). In contrast, the PEGylated AuNPs appeared to enhance the stability of siRNA and provide partial protection from nuclease-mediated degradation (Fig. 5).

In summary, these results suggest that PEGylated AuNPs remain stable in serum avoiding significant aggregation or decomplexation of siRNA for up to 24 h, thus indicating the potential of PEGylated AuNPs to formulate stable delivery systems for siRNA.

3.2.3. Internalisation of PEGylated Gold Nanoparticle.siRNA complexation

Several pathways have been considered to mediate cellular uptake of AuNPs, such as clathrin-mediated endocytosis, caveolae-mediated endocytosis, macropinocytosis, phagocytosis, and direct penetration [37] [38] and [39]. In general, the internalisation of AuNPs can be classified as occurring via either specific (receptor-ligand interaction) or non-specific pathways. For instance, Choi et al. reported that PEGylated AuNPs modified with transferrin (Tf) targeting ligands significantly increased receptor-mediated uptake into cancer cells relative to their nontargeted counterparts [38]. In addition, Verma *et al.* reported that AuNPs modified with two capping molecules (anionic and hydrophobic with alternating positions on the surface) can enter the cells directly (endocytosis-independent entry) without destruction of the cell membrane in a manner similar to cell-penetrating peptides [39] .

In this study, 50 nM of fluorescein-siRNA was used to monitor the internalisation of PEGylated AuNPs containing 'protamine.siRNA' into PC3 cancer cells. Fluorescein-siRNA on its own and complexed with Lipofectamine® 2000 were used as negative and positive controls respectively. Lipofectamine® 2000 achieved approximately 15 % and 65 % fluorescein positive cells at 4 and 24 h post-transfection, respectively (Fig. 6). It has been

previously reported that non-PEGylated G11 containing 20 nM fluorescein-siRNA achieved up to 20% cellular uptake efficiency following 24 h post-transfection [19]. In contrast, the 'protamine.siRNA' (MR0.5) and 'G11 PEG20,000 'protamine.siRNA'' at various mass ratios did not generate significant fluorescein positive cells in comparison to siRNA alone (50 nM) (Fig. 6). The FACS data therefore suggest that PEGylation inhibits the internalisation of AuNPs into cancer cells. A similar lack of cellular internalisation was seen in Hep G2, Caco-2, B16F10 and CT26 cells (data not shown).

Although PEGylation is known to improve *in vitro* and *in vivo* stability and reduce cytotoxicity, it inhibits both the uptake of complexes into tumour cells and the efficient escape from the endosome, thus resulting in low transfection efficacy [40]. To overcome the 'PEG dilemma' phenomenon, tumour-specific ligands such as monoclonal antibodies (mAbs) [41], Tf [42], the Arg-Gly-Asp (RGD) peptide [43] and folic acid [44], can be used to enhance cellular uptake. The design of PEGylated AuNPs in this study provides potential for conjugation of a targeting ligand.

Improved endocytosis of tumour cells due to ligand-receptor mediated internalisation may not be sufficient to produce gene silencing, as NPs are normally entrapped inside endosomal/lysosomal compartments, in which siRNA may be degraded by a variety of degradative enzymes [45]. To enhance endosomal escape of siRNA, microenvironment-responsive materials for example fusogenic peptides, pH-sensitive groups and synthetic polymeric groups have frequently been incorporated into NP formulations [6, 46, 47]. An added advantage of the cysteine-capped AuNPs is the potential of the ammonium groups to promote endosomal escape by a 'proton sponge' effect which results in osmotic swelling and disruption of the endosome thus facilitating release of siRNA into the cytoplasm [48].

4. Conclusion

Despite the therapeutic potential of siRNA, due to the capacity for highly sequence-specific gene downregulation, effective and safe delivery is still a significant barrier to translating the concept into the clinic. Bioengineered AuNPs with different size, shape, structure, chemistry and synthetic strategies have shown potential to enhance siRNA delivery *in vitro* and *in vivo* [15] [16] [49] and [50].

In this study, a series of positively charged, surfactant-free AuNPs decorated with PEG moieties of various molecular weights have been synthesised. The AuNPs with a large core diameter and PEG groups (i.e. GR11 AuNPs-L-cysteine PEG 20,000) demonstrated effective complexation of protamine-complexed siRNA. The resulting formulation showed favorable physicochemical characteristics in terms of size, charge and stability, consistent with requirements for prolonged circulation *in vivo*. PEGylation enhanced the biocompatibility of the AuNPs by reducing toxicity in a range of cell types, by inhibiting interaction with serum proteins thus avoiding aggregation, and, by providing protection against degradation by nucleases. Although PEGylation decreased cellular uptake, the design of the AuNPs can facilitate conjugation of a targeting ligand at the distal end of the PEG chain to enable ligand-receptor mediated internalization thus resulting in effective intracellular trafficking of siRNA into the cytoplasm, and efficient gene silencing (Fig. 7). The attachment of a targeting ligand will be the focus of future work.

Acknowledgements

We acknowledge financial support from Science Foundation Ireland and AMBER (Grant 12/RC/2278) and the Irish Research Council, for a Government of Ireland Postdoctoral Fellowship to Jianfeng Guo (GOIPD/2013/150).

Table 1. Particle size (nm) and zeta potential (mV) of AuNPs with different core sizes with and without PEGylation.

Figure 1. Size distribution (A) and zeta potential (B) for AuNPs-L-cysteine PEG 2,000 with different AuNP core sizes.

Figure 2. Size distribution (A) and zeta potential (B) for GR5 AuNPs-L-cysteine with different PEG molecular weights.

Figure 3. Complexation of ‘protamine.siRNA’ (MR 0.4) with G11 AuNPs-L-cysteine PEG 20,000 at different mass ratios (MRs) using gel retardation (1% agarose gel at 120 mV for 30 min).

Figure 4. Aggregation of ‘G11 AuNPs-L-cysteine ‘protamine.siRNA’’ (A) and ‘G11 AuNPs-L-cysteine PEG 20,000 ‘protamine.siRNA’’ (B) (MR 1:0.4:1) incubated in 50 % FBS for 24 h. Size distribution of serum on its own and complexes incubated in deionised water (DIW) were used as controls. The concentration of siRNA was fixed at 1 μg mL^{-1}.

Figure 5. Serum stability of naked siRNA (0.5 μg), ‘protamine.siRNA’ (MR 0.5) and ‘G11 AuNPs-cysteine PEG 20,000 ‘protamine.siRNA’’ (MR 1:0.4:1) following incubation in 50% FBS for 24 h at 37 °C.

Figure 6. Cellular uptake of naked fluorescein siRNA (50 nM), fluorescein siRNA formulated with Lipofectamine® 2000 or with ‘GR11 AuNPs-L-cysteine PEG 20,000 ‘protamine.siRNA’’ at different mass ratios, analysed by Histogram Plots in PC3 cells by FACS.

Figure 7. A schematic of a multifunctional gold nanoparticle-based delivery vector to improve the internalisation and intracellular trafficking of siRNA in cancer cells. AuNPs allow for flexible chemistry to enable the grafting of a bio-responsive PEG linker and a distal cell-specific targeting ligand. Protamine is used to condensate siRNA into a ‘protamine.siRNA’ core which will improve the complexation with multifunctional AuNPs. When homing to tumour area these ligand-conjugated AuNPs may direct the siRNA delivery into tumour cells via specific cancer cell surface receptors (or antigens), entering into cells by receptor-mediated endocytosis. The endosomal and lysosomal escape of siRNA can be achieved by the activation of bio-responsive groups (i.e. fusogenic peptides, pH-sensitive groups and synthetic polymeric groups).

References:

[1] M. Tuna, C.I. Amos, Cancer Lett, 340 (2013) 161-170.
[2] E. Chan, D.E. Prado, J.B. Weidhaas, Trends Mol Med, 17 (2011) 235-243.
[3] K.A. Fitzgerald, J.C. Evans, J. McCarthy, J. Guo, M. Prencipe, M. Kearney, W.R. Watson, C.M. O'Driscoll, Expert Opin Ther Targets, 18 (2014) 633-649.
[4] R. Kanasty, J.R. Dorkin, A. Vegas, D. Anderson, Nat Mater, 12 (2013) 967-977.
[5] J.E. Dahlman, C. Barnes, O.F. Khan, A. Thiriot, S. Jhunjunwala, T.E. Shaw, Y.P. Xing, H.B. Sager, G. Sahay, L. Speciner, A. Bader, R.L. Bogorad, H. Yin, T. Racie, Y.Z. Dong, S. Jiang, D. Seedorf, A. Dave, K.S. Sandhu, M.J. Webber, T. Novobrantseva, V.M. Ruda, A.K.R. Lytton-Jean, C.G. Levins, B. Kalish, D.K. Mudge, M. Perez, L. Abezgauz, P. Dutta, L. Smith, K. Charisse, M.W. Kieran, K. Fitzgerald, M. Nahrendorf, D. Danino, R.M. Tuder, U.H. von Andrian, A. Akinc, D. Panigrahy, A. Schroeder, V. Koteliansky, R. Langer, D.G. Anderson, Nature Nanotechnology, 9 (2014) 648-655.
[6] J.F. Guo, W.P. Cheng, J.X. Gu, C.X. Ding, X.Z. Qu, Z.Z. Yang, C. O'Driscoll, European Journal of Pharmaceutical Sciences, 45 (2012) 521-532.
[7] J.F. Guo, J.R. Ogier, S. Desgranges, R. Darcy, C. O'Driscoll, Biomaterials, 33 (2012) 7775-7784.
[8] Y. Zhao, C. Zheng, L. Zhang, Y. Chen, Y. Ye, M. Zhao, Colloids Surf B Biointerfaces, 127 (2015) 155-163.
[9] T. Kanazawa, K. Sugawara, K. Tanaka, S. Horiuchi, Y. Takashima, H. Okada, Eur J Pharm Biopharm, 81 (2012) 470-477.
[10] J. Guo, M.R. Cahill, S.L. McKenna, C.M. O'Driscoll, Biotechnol Adv, 32 (2014) 1396-1409.
[11] Y. Xie, H. Qiao, Z. Su, M. Chen, Q. Ping, M. Sun, Biomaterials, 35 (2014) 7978-7991.
[12] J. Guo, J.C. Evans, C.M. O'Driscoll, Trends Mol Med, 19 (2013) 250-261.
[13] W. Lu, G. Zhang, R. Zhang, L.G. Flores, Q. Huang, J.G. Gelovani, C. Li, Cancer research, 70 (2010) 3177-3188.
[14] A.C. Bonoiu, E.J. Bergey, H. Ding, R. Hu, R. Kumar, K.-T. Yong, P.N. Prasad, S. Mahajan, K.E. Picchione, A. Bhattacharjee, Nanomedicine, 6 (2011) 617-630.
[15] S.A. Jensen, E.S. Day, C.H. Ko, L.A. Hurley, J.P. Luciano, F.M. Kouri, T.J. Merkel, A.J. Luthi, P.C. Patel, J.I. Cutler, Sci Transl Med, 5 (2013) 209ra152-209ra152.
[16] J. Conde, F. Tian, Y. Hernández, C. Bao, D. Cui, K.-P. Janssen, M.R. Ibarra, P.V. Baptista, T. Stoeger, J.M. de la Fuente, Biomaterials, 34 (2013) 7744-7753.
[17] D. Zheng, D.A. Giljohann, D.L. Chen, M.D. Massich, X.-Q. Wang, H. Iordanov, C.A. Mirkin, A.S. Paller, Proceedings of the National Academy of Sciences, 109 (2012) 11975-11980.
[18] J. Conde, J. Rosa, J.M. de la Fuente, P.V. Baptista, Biomaterials, 34 (2013) 2516-2523.
[19] J.F. Guo, M.J. Armstrong, C.M. O'Driscoll, J.D. Holmes, K. Rahme, Rsc Adv, 5 (2015) 17862-17871.
[20] J. Guo, K.A. Fisher, R. Darcy, J.F. Cryan, C. O'Driscoll, Mol Biosyst, 6 (2010) 1143-1161.
[21] A.M. O'Mahony, B.M. Godinho, J.F. Cryan, C.M. O'Driscoll, J Pharm Sci, 102 (2013) 3469-3484.
[22] J.V. Jokerst, T. Lobovkina, R.N. Zare, S.S. Gambhir, Nanomedicine (Lond), 6 (2011) 715-728.
[23] K. Rahme, M.T. Nolan, T. Doody, G.P. McGlacken, M.A. Morris, C. O'Driscoll, J.D. Holmes, RSC Advances, 3 (2013) 21016-21024.
[24] K.R. Brown, L.A. Lyon, A.P. Fox, B.D. Reiss, M.J. Natan, Chem Mater, 12 (2000) 314-323.

[25] K. Rahme, L. Chen, R.G. Hobbs, M.A. Morris, C. O'Driscoll, J.D. Holmes, RSC Advances, 3 (2013) 6085-6094.
[26] M.J. O' Neill, J.F. Guo, C. Byrne, R. Darcy, C.M. O' Driscoll, Int J Pharmaceut, 413 (2011) 174-183.
[27] L.D. Unsworth, Z. Tun, H. Sheardown, J.L. Brash, J Colloid Interf Sci, 281 (2005) 112-121.
[28] L.D. Unsworth, H. Sheardown, J.L. Brash, Langmuir, 21 (2005) 1036-1041.
[29] C.M. Goodman, C.D. McCusker, T. Yilmaz, V.M. Rotello, Bioconjugate Chem, 15 (2004) 897-900.
[30] N. Pernodet, X.H. Fang, Y. Sun, A. Bakhtina, A. Ramakrishnan, J. Sokolov, A. Ulman, M. Rafailovich, Small, 2 (2006) 766-773.
[31] S. Vijayakumar, S. Ganesan, Toxicol Environ Chem, 95 (2013) 277-287.
[32] A. Elbakry, A. Zaky, R. Liebl, R. Rachel, A. Goepferich, M. Breunig, Nano Lett, 9 (2009) 2059-2064.
[33] S.D. Li, L. Huang, Mol Pharmaceut, 3 (2006) 579-588.
[34] J.F. Guo, L. Bourre, D.M. Soden, G.C. O'Sullivan, C. O'Driscoll, Biotechnol Adv, 29 (2011) 402-417.
[35] J. Manson, D. Kumar, B.J. Meenan, D. Dixon, Gold Bull, 44 (2011) 99-105.
[36] B.M.D.C. Godinho, J.R. Ogier, A. Quinlan, R. Darcy, B.T. Griffin, J.F. Cryan, C.M. Driscoll, Int J Pharmaceut, 473 (2014) 105-112.
[37] P. Nativo, I.A. Prior, M. Brust, Acs Nano, 2 (2008) 1639-1644.
[38] C.H. Choi, C.A. Alabi, P. Webster, M.E. Davis, Proc Natl Acad Sci U S A, 107 (2010) 1235-1240.
[39] A. Verma, O. Uzun, Y.H. Hu, Y. Hu, H.S. Han, N. Watson, S.L. Chen, D.J. Irvine, F. Stellacci, Nat Mater, 7 (2008) 588-595.
[40] S. Mishra, P. Webster, M.E. Davis, Eur J Cell Biol, 83 (2004) 97-111.
[41] H. Kouchakzadeh, S.A. Shojaosadati, F. Tahmasebi, F. Shokri, Int J Pharm, 447 (2013) 62-69.
[42] Y. Cui, Q. Xu, P.K. Chow, D. Wang, C.H. Wang, Biomaterials, 34 (2013) 8511-8520.
[43] H.A. Kim, K. Nam, S.W. Kim, Biomaterials, 35 (2014) 7543-7552.
[44] S. Duarte, H. Faneca, M.C. Lima, Int J Pharm, 423 (2012) 365-377.
[45] V. Tsouris, M.K. Joo, S.H. Kim, I.C. Kwon, Y.Y. Won, Biotechnol Adv, 32 (2014) 1037-1050.
[46] N. Toriyabe, Y. Hayashi, H. Harashima, Biomaterials, 34 (2013) 1337-1343.
[47] M.-Y. Lee, S.-J. Park, K. Park, K.S. Kim, H. Lee, S.K. Hahn, ACS nano, 5 (2011) 6138-6147.
[48] A.K. Varkouhi, M. Scholte, G. Storm, H.J. Haisma, J Control Release, 151 (2011) 220-228.
[49] S.H. Lee, K.H. Bae, S.H. Kim, K.R. Lee, T.G. Park, International journal of pharmaceutics, 364 (2008) 94-101.
[50] W.H. Kong, K.H. Bae, S.D. Jo, J.S. Kim, T.G. Park, Pharmaceutical research, 29 (2012) 362-374.

Figure(s)

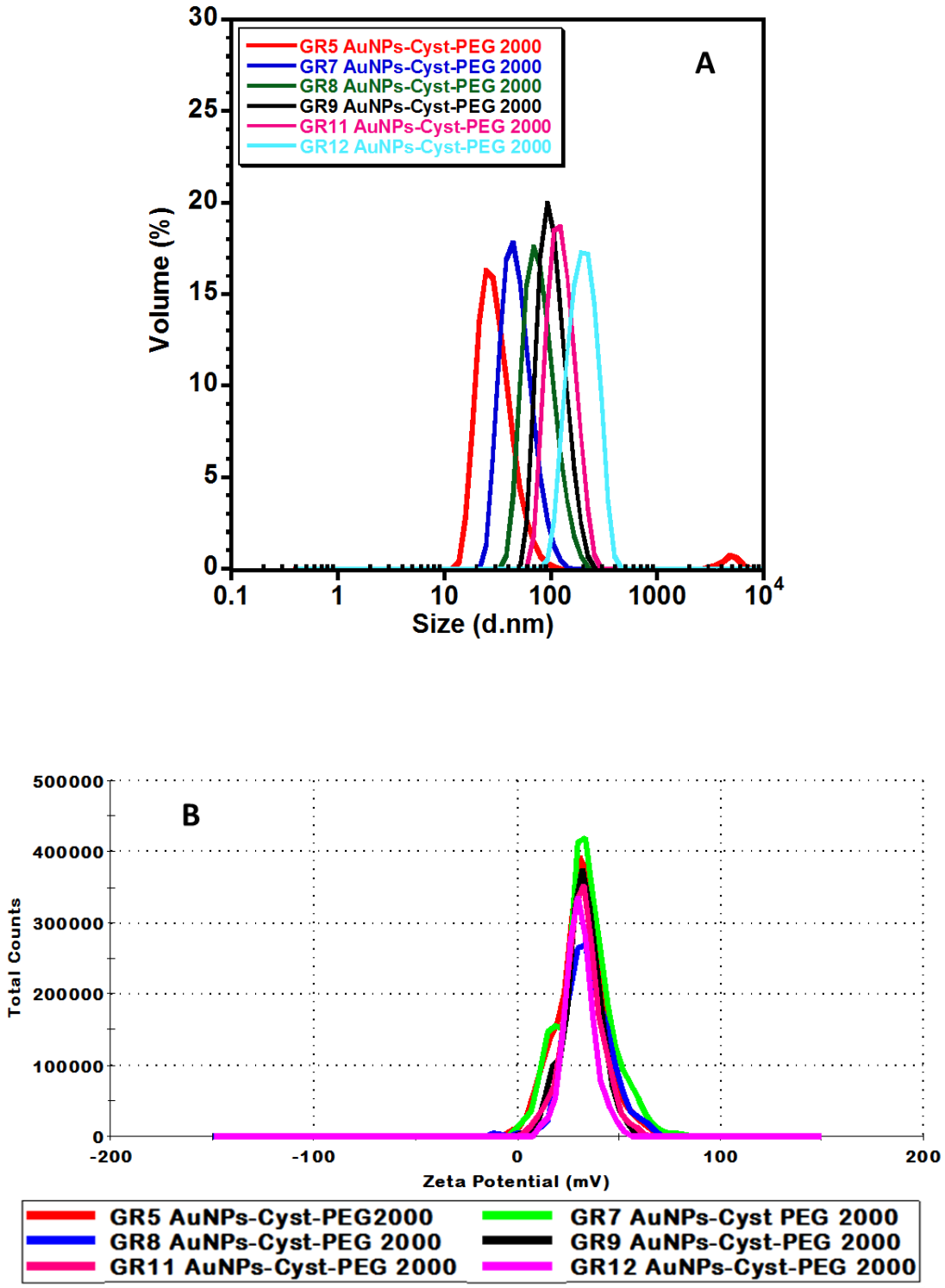

Figure 1. Size distribution (A) and zeta potential (B) for AuNPs-L-cysteine PEG 2,000 with different AuNP core sizes.

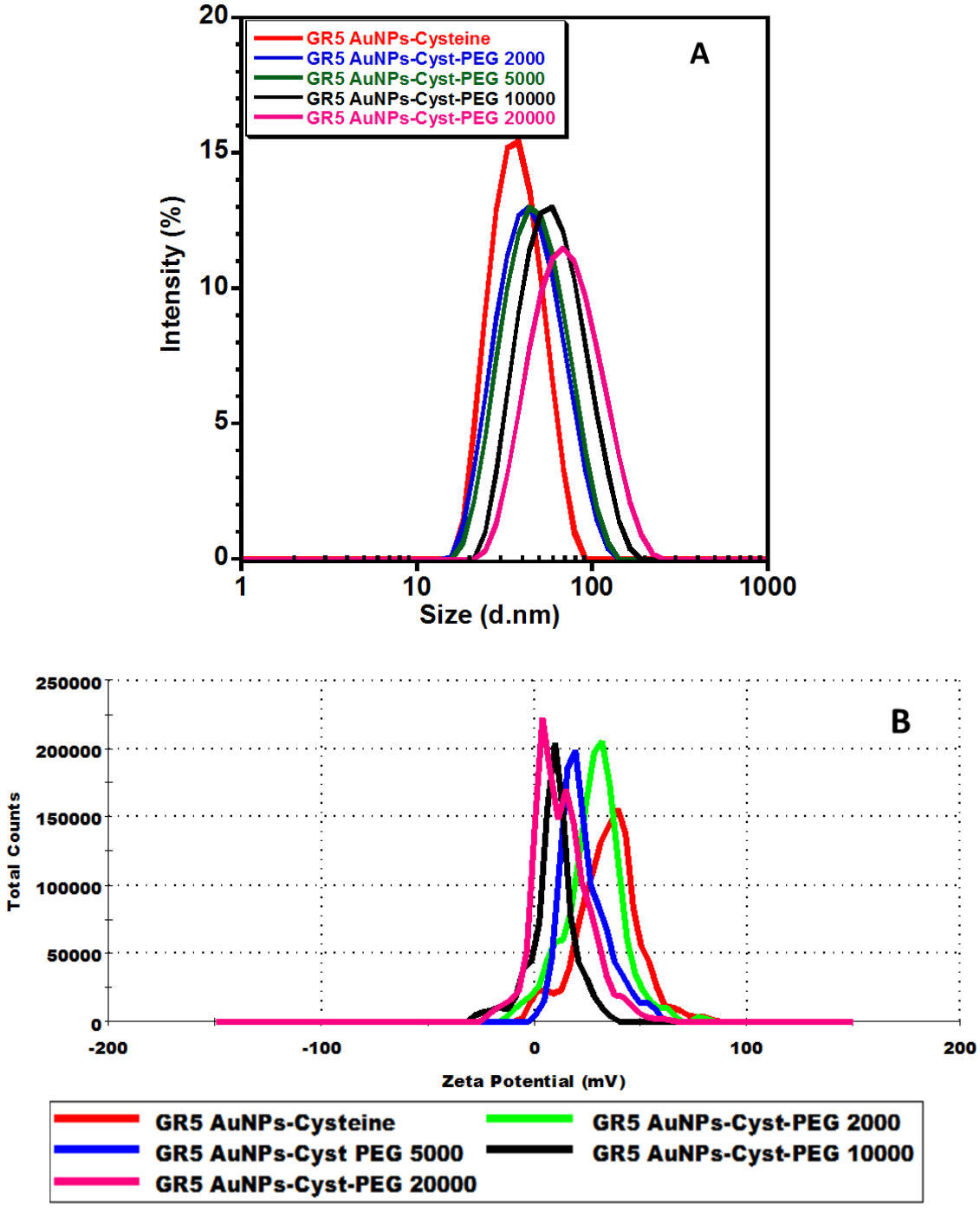

Figure 2. Size distribution (A) and zeta potential (B) for GR5 AuNPs-L-cysteine with different PEG molecular weights.

A = free siRNA (0.5 μg)
B = 'G11 PEG20000 'protamine.siRNA'' (MR = 1 : 0.4 : 1)
C = 'G11 PEG20000 'protamine.siRNA'' (MR = 2 : 0.4 : 1)
D = 'G11 PEG20000 'protamine.siRNA'' (MR = 4 : 0.4 : 1)
E = 'G11 PEG20000 'protamine.siRNA'' (MR = 6 : 0.4 : 1)
F = 'G11 PEG20000 'protamine.siRNA'' (MR = 8 : 0.4 : 1)

Figure 3. Complexation of 'protamine.siRNA' (MR 0.4) with G11 AuNPs-L-cysteine PEG 20,000 at different mass ratios (MRs) using gel retardation (1% agarose gel at 120 mV for 30 min).

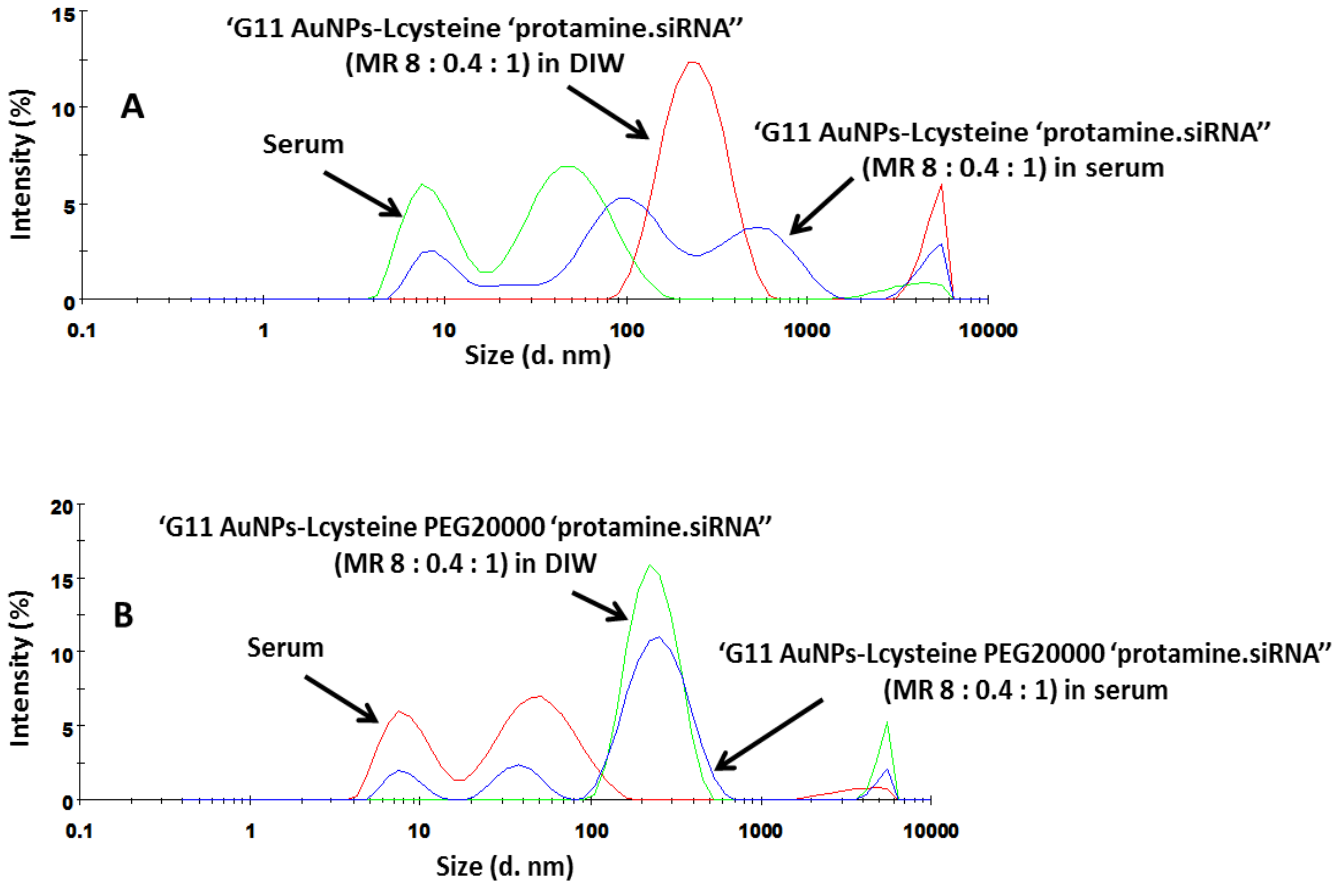

Figure 4. Aggregation of 'G11 AuNPs-L-cysteine 'protamine.siRNA'' (A) and 'G11 AuNPs-L-cysteine PEG 20,000 'protamine.siRNA'' (B) (MR 1:0.4:1) incubated in 50 % FBS for 24 h. Size distribution of serum on its own and complexes incubated in deionised water (DIW) were used as controls. The concentration of siRNA was fixed at 1 µg mL^{-1}.

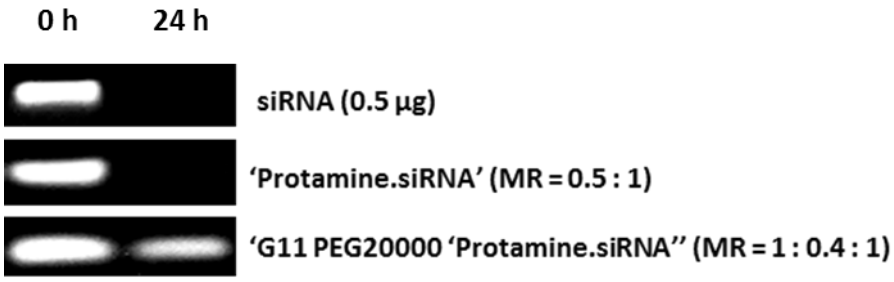

Figure 5. Serum stability of naked siRNA (0.5 µg), 'protamine.siRNA' (MR 0.5) and 'G11 AuNPs-cysteine PEG 20,000 'protamine.siRNA'' (MR 1:0.4:1) following incubation in 50% FBS for 24 h at 37 °C.

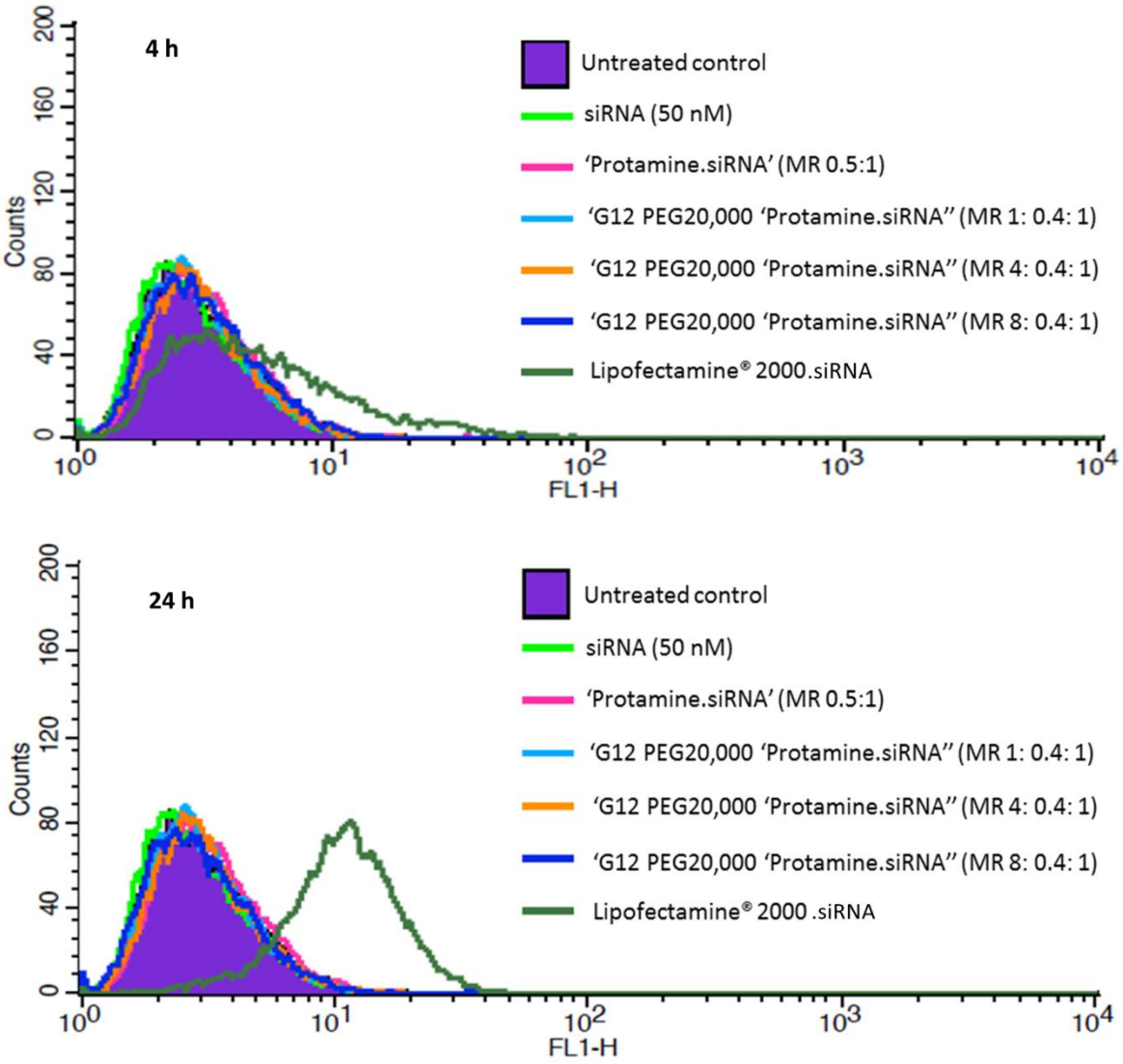

Figure 6. Cellular uptake of naked fluorescein siRNA (50 nM), fluorescein siRNA formulated with Lipofectamine® 2000 or with 'GR11 AuNPs-L-cysteine PEG 20,000 'protamine.siRNA'' at different mass ratios, analysed by Histogram Plots in PC3 cells by FACS.

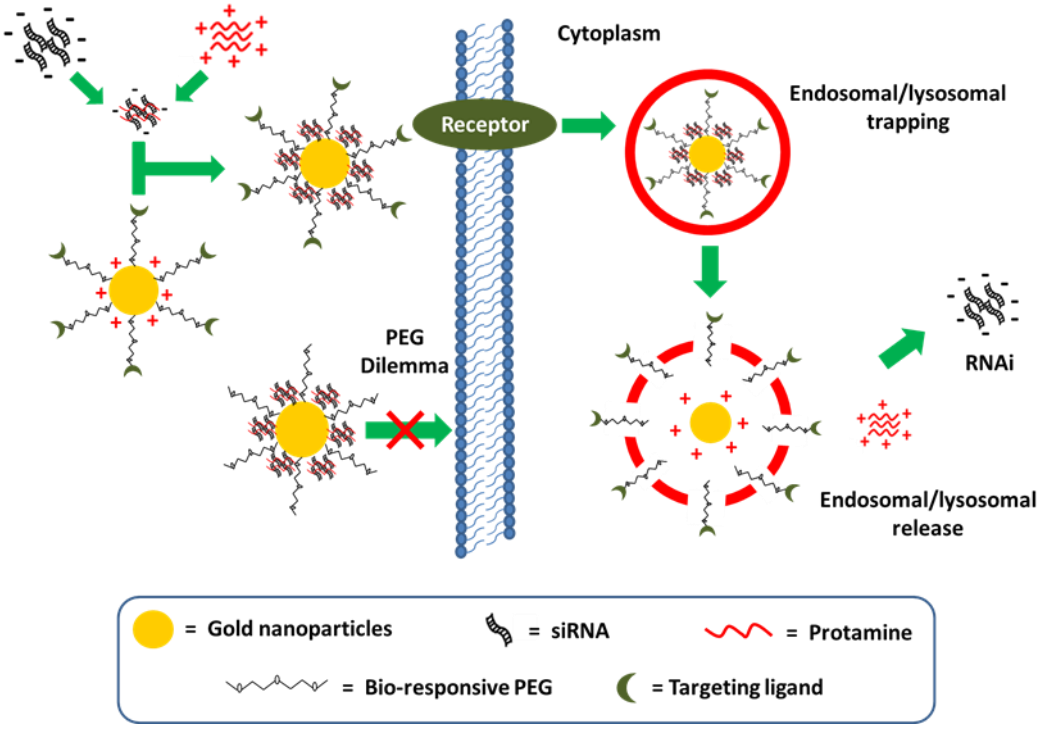

Figure 7. A schematic of a multifunctional gold nanoparticle-based delivery vector to improve the internalisation and intracellular trafficking of siRNA in cancer cells. AuNPs allow for flexible chemistry to enable the grafting of a bio-responsive PEG linker and a distal cell-specific targeting ligand. Protamine is used to condensate siRNA into a 'protamine.siRNA' core which will improve the complexation with multifunctional AuNPs. When homing to tumour area these ligand-conjugated AuNPs may direct the siRNA delivery into tumour cells via specific cancer cell surface receptors (or antigens), entering into cells by receptor-mediated endocytosis. The endosomal and lysosomal escape of siRNA can be achieved by the activation of bio-responsive groups (i.e. fusogenic peptides, pH-sensitive groups and synthetic polymeric groups).

Table(s)

Table 1. Particle size (nm) and zeta potential (mV) of AuNPs with different core sizes with and without PEGylation.

AuNPs	Hydrodynamic Diameter (nm) from DLS / PDI					Zeta Potential (mV) ± Standard Deviation				
	L-cysteine	PEG2000	PEG5000	PEG10000	PEG20000	L-cysteine	PEG2000	PEG5000	PEG10000	PEG20000
GR5	38 / 0.25	47 / 0.23	50 / 0.23	63 / 0.21	76 / 0.36	34.6 ± 14.3	28.1 ± 13.5	23.4 ± 10.7	8.96 ± 10.0	12.8 ± 12.6
GR7	60 / 0.139	64 / 0.12	68 / 0.12	74 / 0.12	77 / 0.12	37.6 ± 16.4	33.5 ± 12.8	29.9 ± 15.2	16.1 ± 11.5	19.8 ± 10.9
GR8	92 / 0.041	97 / 0.09	101 /0.084	110 / 0.083	112 / 0.069	45.4 ± 13.5	34.9 ± 11.2	29.0 ± 11.6	12.4 ± 9.11	16.1 ± 9.37
GR9	113 / 0.108	116 / 0.09	118 / 0.034	124 / 0.125	129 / 0.071	44.3 ± 11.8	32.0 ± 9.02	28.5 ± 11.4	14.2 ± 8.90	15.8 ± 10.5
GR11	136 / 0.07	143 / 0.08	137 / 0.04	150 / 0.07	156 / 0.06	41.6 ± 11.1	32.1 ± 9.30	35.0 ± 13.6	10.0 ± 10.4	9.38 ± 6.37
GR12	191 / 0.19	196 / 0.03	203 / 0.09	212 / 0.09	218 / 0.07	41.2 ± 10.8	30.08 ± 7.02	31.6 ± 9.23	10.6 ± 7.17	8.85 ± 7.03